Acta Polytechnica CTU Proceedings **54**:23–28, 2025
https://doi.org/10.14311/APP.2025.54.0023

Published by the Czech Technical University in Prague

FRACTIONAL CALCULUS IN DESCRIBING THE VISCOELASTIC RESPONSE OF PVB FOIL

Barbora Hálková*, Michal Šejnoha

Czech Technical University in Prague, Faculty of Civil Engineering, Department of Mechanics, Thákurova 7, 166 29 Praha 6, Czech Republic

* corresponding author: barbora.halkova@fsv.cvut.cz

Abstract. To address the response of a PVB foil, both traditional and fractional viscoelasticity based formulations are described and compared in this paper. Traditional viscoelasticity uses models consisting of elastic springs and viscous dashpots. Fractional viscoelasticity is based on the principles of fractional calculus (derivatives and integrals of non-integer order) and introduces another rheological element, the springpot, which behaves as viscoelastic on its own and allows us to construct even more complex models. While limiting attention to the Maxwell chain model, both formulations are compared in light of approximation of experimental data provided by rheometer measurements. This is illustrated by plotting the storage modulus derived experimentally as well as computationally, which in turn promotes application of fractional calculus as an efficient tool for smoothing out and storing the experimental data.

Keywords: Viscoelasticity, fractional viscoelasticity, springpot, generalized Maxwell model, laminated glass, PVB foil, rheometer experiment.

1. Introduction

A number of engineering materials, including concrete, bitumen, polymers or even human skin tissue, show viscoelastic properties. The present paper focuses on the behaviour of polyvinyl butyral (PVB) thermoplastic polymer with a particular application in laminated glass panels. Laminated glass is a composite material which consists of glass plates and transparent polymer interlayers, both varying in properties and thicknesses. The interlayer ensures an interaction between the individual glass plates and has also an important safety function ensuring that in case of fracture the glass shards remain stuck to the interlayer.

The behaviour of viscoelastic materials non-negligibly depends on time. With reference to concrete structure we are generally concerned with creep describing an increasing deformation over time under constant load. Relaxation, on the other hand, represents a continuous decrease of internal stress over time while the strain remains unchanged. This might be a key factor when designing a precast steel reinforcement.

To address viscoelastic materials the models combining elastic and viscous elements are used. The presented research endeavour attempts to compare this traditional approach with fractional viscoelasticity. The latter approach is based on fractional calculus which introduces the theory of derivatives and integral of non-integer order.

The remainder of the paper is organized as follows. Section 2 provides a brief review of theoretical grounds of both traditional and fractional viscoelasticty. The results of experimental measurements together with calibration of corresponding Maxwell chain models are presented in Section 3. The essential concluding remarks are then summarized in Section 4.

2. Theory of viscoelasticity

A viscoelastic material, as the name suggests, experiences both elastic and viscous properties. The behaviour of such a material is bounded by two limit cases – pure elasticity and pure viscosity.

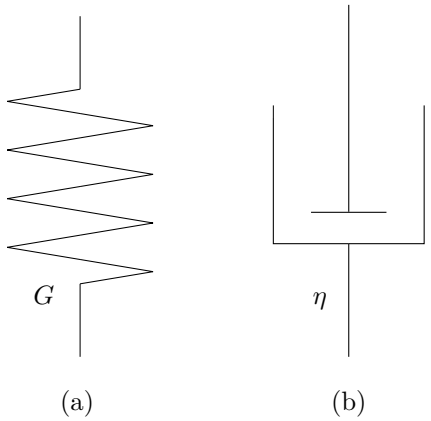

Figure 1. Elastic spring (a) and viscous dashpot (b).

Purely elastic material is commonly modelled by a linear spring, see the rheological scheme in Figure 1(a). The associated mathematical representation corresponds the Hooke law which, in the domain of shear response, reads

$$\tau = G\gamma. \tag{1}$$

This law prescribes a linear relationship between the shear stress τ and the shear strain γ. The proportionality is given by the shear modulus of elasticity

G, the material property which we consider constant over time.

The response of spring depends on the load only and is independent of time unless the load changes – instantaneous constant stress load causes immediate increase of strain, there is no additional increase or decrease of strain over time. The same applies to an instantaneous loading by a constant strain which manifests by an immediate change of internal stress remaining constant ever since. Removing the load also causes the corresponding response to disappear – the spring returns to its original state before the load was applied. For illustration, the elastic response to a constant unit stress load is depicted by the brown line in Figure 2 and the response to a constant unit strain load in Figure 3.

Purely viscous material, on the other hand, is modelled by a viscous dashpot, see the scheme in Figure 1(b). Its behaviour is described by the Newton law of viscosity which has the following form

$$\tau = \eta\dot{\gamma}. \tag{2}$$

We observe a linear relationship between the shear stress τ and the first time derivative of shear strain, i.e., the shear strain rate $\dot{\gamma}$. The proportionality coefficient is represented by the coefficient of viscosity η (considered constant over time).

In the case of viscous dashpot, an instantaneous constant stress load leads to an immediate change of strain rate which results in a linear increase of strain over time. Therefore, the response of the viscous dashpot is time dependent – the longer the stress load is acting, the larger the deformation of the element is. Removing the load causes the strain rate to return back to zero but the deformation does not disappear. It remains constant over time unless the opposite stress load is applied. Loading the dashpot by an immediate constant strain would require an infinite strain rate at the onset of its application which in turn would cause an infinite internal stress of the element. Passing this moment the strain remains constant and the strain rate and the stress become zero. The viscous response to a constant unit stress and strain load, respectively, is depicted by the pink line in Figures 2–3.

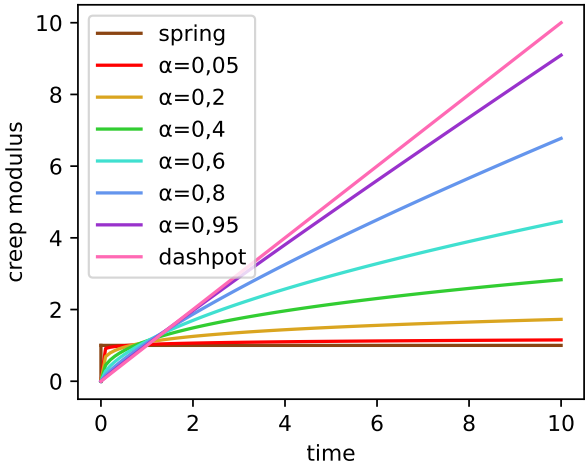

Figure 2. Creep modulus of springpot in dependence on parameter α.

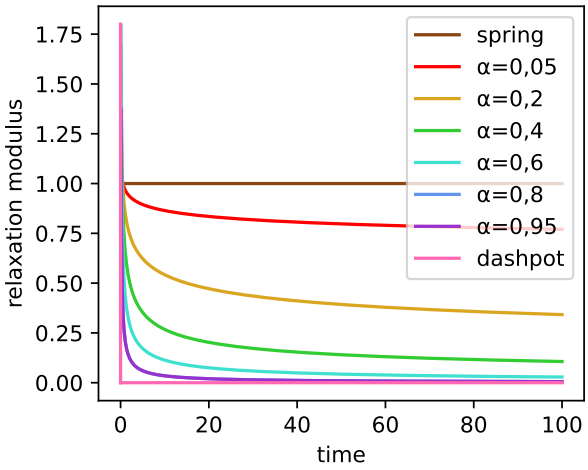

Figure 3. Relaxation modulus of springpot in dependence on parameter α.

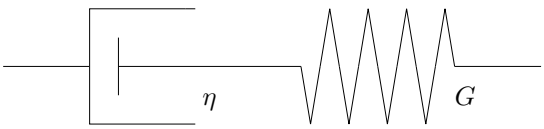

Figure 4. Maxwell model.

2.1. Traditional viscoelasticity

As was mentioned above, the viscoelastic material behaves somewhere between the two limit cases given by ideal elasticity and viscosity. To describe a viscoelastic material it is standard to use springs and dashpots to compose more complex models by connecting them together in series or in parallel. These models then possess both elastic and viscous properties given by the properties and types of connection between individual elements.

There are endless possibilities how to construct a viscoelastic model using springs and dashpots. One of the most simple models is the Maxwell model (also referred to as the Maxwell cell), which consists of one spring and one dashpot connected together in series, see the scheme in Figure 4.

Loading the model by an instantaneous constant stress would cause an immediate deformation of the spring followed by a linear increase of the deformation of dashpot. Upon removing the load the elastic deformation disappears and the viscous deformation of dashpot remains constant. This example shows that by jointly employing the spring and the dashpot provides a model that combines the elastic and viscous response, it therefore behaves as viscoelastic.

The properties of the Maxwell model are specified by its two parameters – the shear modulus of elasticity G and the coefficient of viscosity η. Their ratio is called

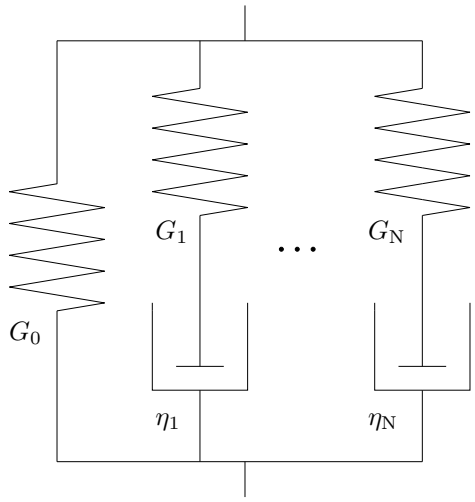

FIGURE 5. Generalized Maxwell chain model.

the characteristic time

$$\tau_c = \frac{\eta}{G}, \tag{3}$$

which represents the time when the increasing viscous deformation reaches the same value as the elastic one under the constant stress load.

The applicability of several theoretical models for the description of a PVB foil is thoroughly discussed in [1]. It was suggested that one of the most suitable models is the generalized Maxwell chain model. This model consists of a single spring connected in parallel with N Maxwell cells, see the scheme in Figure 5.

2.2. Fractional viscoelasticity

Fractional viscoelasticity is based on the theory of integrals and derivatives of non-integer order. The principle of fractional integration generalizes the Cauchy formula for n-times repeated integration

$$I^n f(x) = \frac{1}{(n-1)!}\int_0^x (x-y)^{n-1} f(y)\mathrm{d}y, \tag{4}$$

where I^n denotes an integral operator of order $n \in \mathbb{N}$. Generalizing the factorial function into the gamma function Γ allows us to introduce the Riemann-Liouville fractional integral

$$I^\alpha f(x) = \frac{1}{\Gamma(\alpha)}\int_0^x (x-y)^{\alpha-1} f(y)\mathrm{d}y, \tag{5}$$

where I^α denotes an integral operator of non-integer order $\alpha \in \mathbb{R}$. The definition of the fractional integral leads us to the two most commonly used definitions of the fractional derivative.

The Caputo fractional derivative is defined as follows

$$D^\alpha f(x) = I^{\lceil\alpha\rceil-\alpha}\left[D^{\lceil\alpha\rceil} f(x)\right], \tag{6}$$

where $\lceil\alpha\rceil$ denotes the ceiling function. For example, to obtain the 0.8^{th} derivative of function $f(x)$ we take its first derivative and then integrate the result 0.2 times.

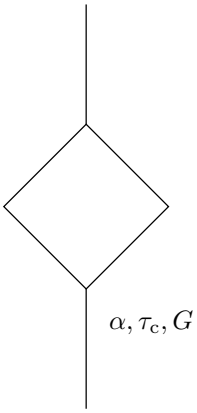

FIGURE 6. Springpot.

The Riemann-Liouville fractional derivative is prescribed as

$$D^\alpha f(x) = D^{\lceil\alpha\rceil}\left[I^{\lceil\alpha\rceil-\alpha} f(x)\right]. \tag{7}$$

Both of these definitions lead to the same final results. A broader insight into fractional calculus can be found in [2, 3], to cite a few.

The fractional calculus allows us to introduce another rheological element, a springpot, see the scheme in Figure 6. The constitutive law for the springpot element has the following form

$$\tau(t) = \xi D^\alpha \gamma(t), \tag{8}$$

where ξ and α are the model parameters of the springpot.

The springpot shows proportionality between the stress and the non-integer α-th derivative of strain. For better understanding of the parameters of springpot, the parameter ξ can be rewritten with the help of characteristic time as

$$\xi = G\tau_c^\alpha. \tag{9}$$

Substituting this representation into Eq. (8) gives

$$\tau(t) = G\tau_c^\alpha D^\alpha \gamma(t). \tag{10}$$

For the application in the theory of viscoelasticity the limit cases given by pure elasticity and pure viscosity have to be respected. These limit cases are now obvious from Eq. (10). For $\alpha = 0$ we get the following equation

$$\tau(t) = G\tau_c^0 D^0 \gamma(t) = G\gamma(t), \tag{11}$$

which is identical to the Hooke law describing the behaviour of a purely elastic material, recall Eq. (1). For $\alpha = 1$ we receive

$$\tau(t) = G\tau_c^1 D^1 \gamma(t) = \eta\dot{\gamma}(t), \tag{12}$$

which corresponds to the Newton law of viscosity introduced in Eq. (2).

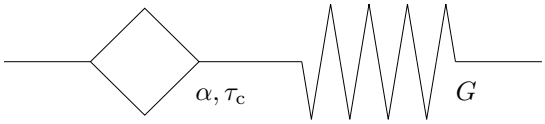

Figure 7. Fractional Maxwell model.

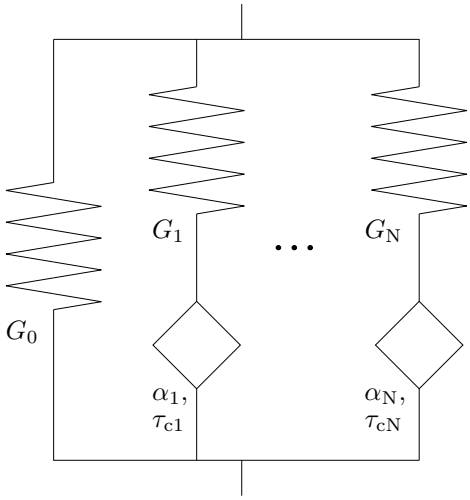

Figure 8. Fractional Maxwell chain model.

Figure 9. Dynamic shear rheometer Malvern KINEXUS DSR+.

The behaviour of springpot is therefore strongly dependent on its parameter α. This dependence is illustrated in the following graphs. Figure 2 shows the time evolution of strain due to unit stress load (i.e. the creep modulus). Figure 3 then plots the stress response to a unit strain load (i.e. the relaxation modulus). In both graphs the limit cases of pure elastic and pure viscous response are displayed together with the response of a single springpot with varying parameter α. It is evident that reducing the parameter α down to zero brings the response closer a purely elastic material (the brown line in the graph). On the other hand, when the parameter α approaches one, the springpot element becomes to approximate a purely viscous material (the pink line in the graph).

The springpot element on its own behaves as viscoelastic. However, a single springpot element is not sufficient to describe most of the viscoelastic materials and it is necessary to introduce more complex rheological models. The standard Maxwell model was already presented earlier in this paper. By replacing the viscous dashpot with the viscoelastic springpot the fractional Maxwell model (fractional Maxwell cell) is obtained, see the rheological scheme in Figure 7. Connecting more fractional Maxwell cells together with a single spring then forms the fractional Maxwell chain model, see Figure 8.

Compared to the standard Maxwell model the fractional model has more parameters. While for the standard model we need two parameters to specify its behaviour (the shear modulus G and either the viscosity coefficient η or the characteristic time τ_c), the behaviour of the fractional model yet depends on the springpot parameter α amounting to three parameters to be identified. The standard Maxwell chain of N cells has then $2N + 1$ free parameters (G_i and η_i for each cell and the modulus of the single spring G_0). For the fractional Maxwell chain we arrive at $3N + 1$ free parameters.

3. Calibration of theoretical models

The Maxwell chain in its standard as well as its fractional form was deem suitable for the description of PVB foil. To describe this material properly requires calibration of free model parameters to fit experimental measurements computationally. For this purpose, an extensive experimental program exploiting the dynamic shear rheometer Malvern KINEXUS DSR+ in Figure 9 was executed to examine the response of PVB foils with variable thicknesses. By loading the sample in a simple torsion the device determines both elastic and viscous properties of the material, see also [4] for further details.

In the rheometer the sample is attached between the two parallel plates as is shown in Figure 10. The bottom plate is fixed while the upper plate can move along and rotate around its vertical axis.

The sample is loaded by a harmonic (sinusoidal) shear strain while the stress response is monitored by the rheometer. The software then extracts the values of amplitudes of the strain γ_0 and the stress τ_0 and the phase shift δ between the load and the response.

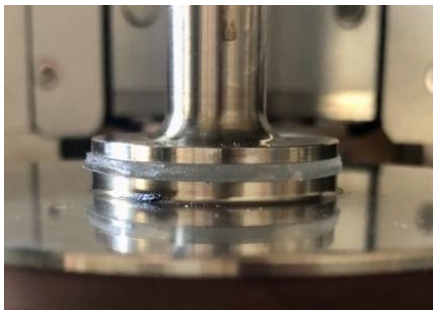

FIGURE 10. Sample attached to parallel-plate rheometer.

These values are converted into the required outputs – the storage modulus G', the loss modulus G'', and the complex modulus G^*. These moduli are given by

$$\begin{aligned} G'(\omega) &= \frac{\tau_0}{\gamma_0}\cos\delta, \\ G''(\omega) &= \frac{\tau_0}{\gamma_0}\sin\delta, \\ G^*(\omega) &= G'(\omega) + iG''(\omega). \end{aligned} \tag{13}$$

The rheometer outputs are based on the known diameter of the rheometer plates and the gap between the plates, which corresponds to the thickness of the sample with the assumption of the sample perfectly filling the gap between the plates.

The behaviour of PVB is strongly dependent on time and temperature and therefore the measurements were performed for several different frequencies and temperatures and also for two different thicknesses of the material sample, 0.76 and 1.52 mm in particular. We observed some differences in the response of the two types of specimens suggesting the need of their separate calibration. The detailed description of the experiment along with the complete set of results can be found in [5]. Here, only the results pertinent to 0.76 mm sample are presented to compare the predictions provided by the standard and fractional viscoelasticity.

Mathematically, the storage modulus of the standard Maxwell chain has the following form

$$G'(\omega) = G_0 + \sum_{i=1}^{N} \frac{G_i \omega^2 \tau_{ci}^2}{\omega^2 \tau_{ci}^2 + 1}, \tag{14}$$

whereas the storage modulus associated with the fractional model reads

$$G'(\omega) = G_0 + \sum_{i=1}^{N} G_i \frac{\beta_i^2 + \beta_i \cos\left(\alpha_i \frac{\pi}{2}\right)}{\beta_i^2 + 2\beta_i \cos\left(\alpha_i \frac{\pi}{2}\right) + 1}, \tag{15}$$

where $\beta_i = (\tau_{ci}\omega)^{\alpha_i}$.

It is obvious that the behaviour of the model depends on the number of cells N. In general, the higher the number of cells, the more accurate approximation of the experimental data can be achieved. However,

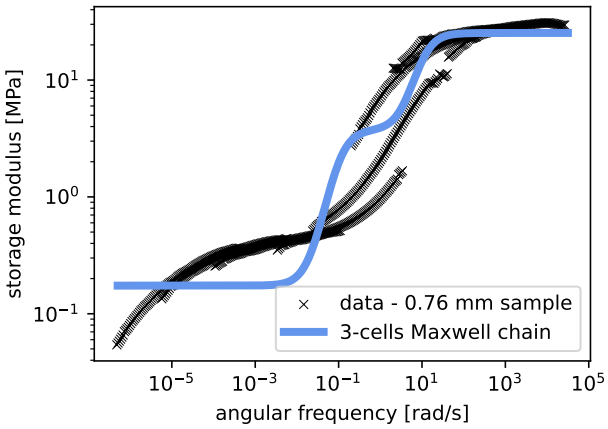

FIGURE 11. Calibration – 3-cells standard Maxwell chain vs experimental data.

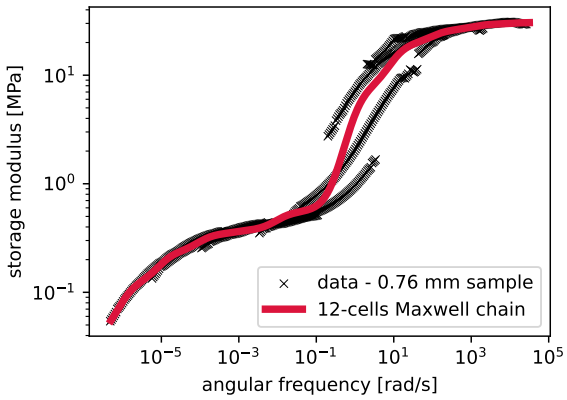

FIGURE 12. Calibration – 12-cells standard Maxwell chain vs experimental data.

with the increasing number of cells the number of model parameters that need to be calibrated also increases. It is, therefore, necessary to find compromise between accuracy and efficiency.

For better illustration see Figures 11–12 which show predictions via the calibrated standard Maxwell chain model with various number of cells. The black crosses represent the data obtained from the rheometer experiment. The blue line in Figure 11 is the approximation of the measured data by the 3-cells standard Maxwell chain model (this model has therefore 7 parameters in total). It is obvious that this approximation is not accurate enough and the number of cells need to be higher. A suitable approximation was obtained using 12-cells standard Maxwell chain model (37 parameters in total), see the red line in Figure 12.

Table 1 lists the corresponding stiffnesses found for the selected characteristic times assumed to be uniformly distributed as

$$\tau_{ci} = 10^j, \quad j = -5, -4, \ldots, 6, N = 12. \tag{16}$$

The approximation provided by the fractional model is presented in Figure 13 suggesting better fitting capabilities with smaller number of model parameters, see the green line representing the 3-cells fractional

Modulus	Value	Modulus	Value
G_0	0.03733	G_7	1.139e-07
G_1	2.067e-07	G_8	7.309
G_2	0.0870	G_9	11.9472
G_3	0.1149	G_{10}	6.3631
G_4	0.1101	G_{11}	3.401
G_5	0.02511	G_{12}	1.0174
G_6	0.1788		

Table 1. Spring moduli in [MPa] of standard Maxwell chain – 0.76 mm sample, fitting to experimental data.

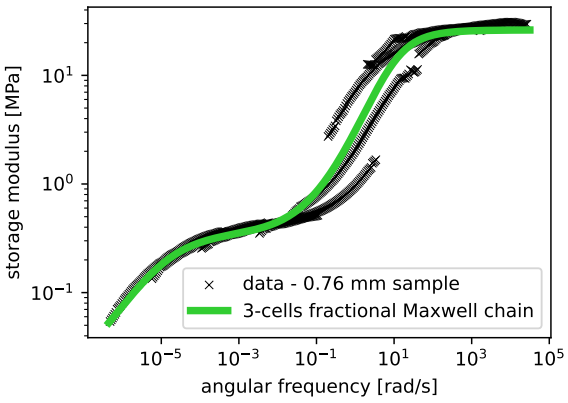

Figure 13. Calibration – 3-cells fractional Maxwell chain vs experimental data.

Maxwell chain with 10 parameters in total including the characteristic times whose choice, however, is not as straightforward as in the case of standard model. As evident from Figure 14, the 3-cells fractional model provides a considerably smoother yet more accurate approximation of experimental data in comparison to the 12-cells standard model.

The resulting set of optimal parameters is provided in Table 2 for the characteristic times selected as

$$\tau_{ci} = 10^j, \quad j = -2, 2, 5, N = 3. \tag{17}$$

4. Conclusion

This paper introduces the principles of fractional viscoelasticity and compares the traditional approach with the fractional one to describe the response of a PVB foil. The traditional viscoelasticity employs theoretical models based on elastic springs and viscous dashpots. The fractional viscoelasticity introduces the viscoelastic springpot element. This approach requires more demanding mathematical background including the derivatives and integrals of non-integer order and it operates with more complicated analytical formulas.

Although analytical operations with the fractional models are more complicated, their application in the approximation of experimental data offer undoubtedly some advantages. The essential one is seen in smoothing the experimental data with strong fitting power even at both tails of the master-curve with a relatively

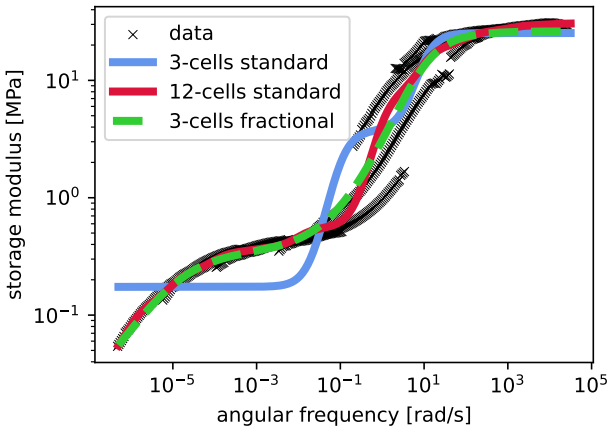

Figure 14. Calibrated theoretical models vs experimental data.

Modulus	Value [MPa]	Parameter	Value
G_0	0.007426	α_1	0.7043
G_1	25.7932	α_2	0.4625
G_2	0.05564	α_3	0.5241
G_3	0.3438		

Table 2. Parameters of fractional Maxwell chain – 0.76 mm sample, fitting to experimental data.

low number of cells. Such a smooth approximation can be then adopted in the calibration of the standard Maxwell chain, which still appears more suitable in structural analyses, e.g., in the combination with finite element method.

Acknowledgements

This publication was supported by the Czech Science Foundation, the grant No. 22-15553S and by the Grant Agency of the Czech Technical University in Prague, grant No. SGS24/038/OHK1/1T/11.

References

[1] B. Hálková. *Viskoelastic description of polymer interlayer of laminated glass.* Bachelor's thesis, Czech Technical University In Prague, 2022.

[2] K. Oldham, J. Spanier. *The fractional calculus theory and applications of differentiation and integration to arbitrary order.* Elsevier, 1974.

[3] L. C. Becker, İ. K. Purnaras. Fractional relaxation equations and a Cauchy formula for repeated integration of the resolvent. *Advances in the Theory of Nonlinear Analysis and its Application* **2**(1):11–32, 2018. https://doi.org/10.31197/atnaa.379282

[4] T. Hána, T. Janda, J. Schmidt, et al. Experimental and numerical study of viscoelastic properties of polymeric interlayers used for laminated glass: Determination of material parameters. *Materials* **12**(14):2241, 2019. https://doi.org/10.3390/ma12142241

[5] B. Hálková. *Experimental and numerical modelling of PVB foil.* Master's thesis, Czech Technical University In Prague, 2024.